



An in Vitro Study on Anticancer Efficacy of Capecitabine- and Vorinostat-incorporated Self-nanoemulsions

Razieh Nazari-Vanani (PhD)¹, Naghmeh Sattarahmady (PhD)^{1,2}, Khashayar Karimian (PhD)³, Hossein Heli (PhD)^{1*}

¹Nanomedicine and Nanobiology Research Center, Shiraz University of Medical Sciences, Shiraz, Iran

²Department of Medical Physics, School of Medicine, Shiraz University of Medical Sciences, Shiraz, Iran

³Arasto Pharmaceutical Chemicals Inc., Yousefabad, Jahanarar Avenue, Tehran, Iran

ABSTRACT

Background: Cancer has emerged as a critical global health concern due to its widespread prevalence and impact on individuals, families, communities, and health-care systems worldwide.

Objective: We investigated the anticancer effectiveness of capecitabine (CAP) and vorinostat (VOR) when incorporated into self-nanoemulsifying drug delivery systems (SNEDDSs).

Material and Methods: In this experimental study, the SNEDDSs were formulated using polyethylene glycol 600 (PEG 600), castor oil and Tween 80. A ternary phase diagram was plotted for the SNEDDSs components and the single-phase formation region was attained. SNEDDSs were then prepared by dilution of the selected ratios of these components in water. Blank SNEDDSs containing ratios (in weight) of castor oil:Tween 80:PEG 600 of 50:30:20 (S1-SNEDDS) and 25:15:60 (S2-SNEDDS) were selected. S1-SNEDDS was loaded with CAP (S1-SNEDDS-CAP), and S2-SNEDDS was loaded with VOR (S2-SNEDDS-VOR).

Results: The developed SNEDDSs formed oil nanodroplets without phase separation. Using dynamic laser light scattering, S1-SNEDDS, S2-SNEDDS, S1-SNEDDS-CAP and S2-SNEDDS-VOR had droplets with average sizes of 171 ± 37 , 82 ± 18 , 117 ± 26 and 37 ± 8 nm, respectively, accompanied by span values of 0.96, 0.95, 0.97 and 0.96, respectively. CAP and VOR were effectively loaded into the SNEDDSs with high entrapment efficiencies and loading capacities. Considerable improvements in cells viability for CAP and VOR were attained upon loading into SNEDDSs. TUNEL assays of the cells upon treatment by S1-SNEDDS-CAP and S2-SNEDDS-VOR revealed a significant apoptosis in all the cells.

Conclusion: The study provides valuable insights into the potential of utilizing SNEDDSs as a novel delivery system for improving the anticancer properties of CAP and VOR.

Keywords

Zolinza; 5-Deoxy-5-Fluorouridine; Deacetylase Inhibitor; Nanoemulsion; Anticancer Efficacy; Drug Delivery Systems; Phase Separation; MCF7 Cells; PANC1 Cells; Hela Cell Lines

Introduction

Cancer has become one of the most important global health issues. The less developed countries are more severely affected because of unavailability and unaffordability of anti-cancer drugs (The *Economist Technology Quarterly*, Treating Cancer, Sept. 16, 2017,

*Corresponding author:
Hossein Heli
Nanomedicine and Nanobiology Research Center, Shiraz University of Medical Sciences, Shiraz, Iran
E-mail:
hheli7@yahoo.com

Received: 4 May 2024
Accepted: 15 July 2024

1-12). About 7.6 million people succumb to cancer annually [1]. Many current anticancer drugs suffer from low efficacy, including sub-optimal therapeutic activity and dose-limiting side effects. These shortcomings lead to poor life quality and low patient compliance to available therapies [2]. Breast, cervix, and pancreatic cancers are causes of death in less developed countries [3]. Many anticancer drugs are used as single or in combination therapies [1]. For example, capecitabine (CAP) as a fluoropyrimidine carbamate is administrated for cancer treatment which is resistant to first line chemotherapy drugs [4]. CAP is a prodrug of 5-fluorouridine which undergoes a series of enzymatic reactions to afford 5-fluorouracil, which in turn inhibits thymidylate synthase thereby preventing the biosynthesis of thymidine monophosphate requiring for *de novo* biosynthesis of DNA [5]. It therefore mimics pharmacodynamic responses through acting as a nutrient of normal cells needed to growth of cancer cells [6]. Generally, conventional dosage form of CAP produces unwanted outcomes such as hand-foot syndrome, diarrhea, myocardial infarction, nausea, angina, anemia, hyperbilirubinemia, thrombocytopenia and stomatitis [7]. Hence, novel therapeutic routes are needed to develop so that all types of cancers can be treated.

Histone deacetylase inhibitors (HDACIs) are the other category of drugs. They induce cell cycle arrest, inhibit proliferation of cells, promote apoptosis, and induce differentiation in many of solid and hematological malignancies [8]. Several HDACIs have been shown that cause death of cancer cells *in vitro* as well as *in vivo* [9]. Vorinostat (VOR, also known as SAHA or Zolinza) is an inhibitor of HDACIs, induce growth arrest and promote apoptosis in a variety of cancer cell lines [10].

VOR therapy is effective but suffers from certain drawbacks such as side effects, poor solubility leading to reduced bioavailability and thus reduced efficacy [11].

Recently, because of their ability to deliver

drugs, designed nanostructures have been proposed as components of cancer treatment platforms [12]. Such systems are characterized by special features including a high ratio of surface area to mass, high surface (re) activity, modified physicochemical properties such as changed solubility, and flexible surface chemistry [13]. The benefits of these drug delivery systems include multitherapy capability, prolonged half-life and efficient delivery of ingredients, limited resistance by efflux pump bypassing and targeting special cancer cells [14]. In the past years, nanomaterials offer numerous applications in medicine [15-20]. Nanoformulations including nanoemulsions [21], dendrimers [22], liposomes [23], nanoparticles [24], and polymeric micelles [25] have been employed as the foundation of drug delivery vehicles.

Self-nanoemulsifying drug delivery systems (SNEDDSs) have had tremendous interest because of the potential to reduce unwanted side effects, enhance the efficacy of chemotherapeutic agents, and afford greater efficiency and safety [26]. A SNEDDS is an isotropic mixture of an oil, a surfactant, and a cosurfactant [27]. When a SNEDDS is placed in contact with an aqueous media, it spontaneously forms fine oil nanodroplets as a nanoemulsion. So far, three marketed SNEDDS have emerged including Norvir® (ritonavir), Neoral® (cyclosporin A) and Fortovase® (saquinavir) [28]. In our previous works, we showed the improved solubility and efficiency of drugs with nanoemulsions [21].

The evaluation of the efficacy of CAP and VOR on different cancer cell lines has been recently approached [7, 14, 29-41].

VOR-incorporated nanoparticles have been synthesized to improve the drug's anticancer activity against human cholangiocarcinoma cells [42]. In another study, CAP and 5-fluorouracil have been used and the results indicated that the MCF7 cell line had no response to CAP within 24 h [43]. However, after 48 h treatment of MCF7 cell line with

CAP with a concentration of 1.15 mg mL⁻¹, 50% of cells were killed. Kwak et al. prepared a nanofiber membrane on a gastrointestinal stent surface with incorporating VOR. Released VOR from nanofibers and VOR alone were used to assess anticancer activity against cholan-giocarcinoma cells. Cell viability was reduced depend on the VOR concentration in the nanofibers [42]. In another study, VOR was loaded into solid lipid nanoparticles and coated with hyaluronic acid [44]. The formulation showed more cytotoxicity than free VOR or VOR-loaded solid lipid nanoparticles alone in A549 and SCC-7 cells.

We have not found report on CAP- and VOR-loaded SNEDDSs. In the present study, SNEDDSs loaded with CAP and VOR were prepared from polyethylene glycol 600 (PEG 600), castor oil and Tween 80 were evaluated. To prepare SNEDDSs, a ternary phase diagram was firstly constructed, and the SNEDDSs were characterized by particle size analysis (PSA) as well as field emission scanning electron microscopy (FESEM). The formulation cytotoxicity was assayed against MCF7, PANC1 and HeLa cell lines and compared with cytotoxicity of CAP and VOR.

Material and Methods

Materials

In this experimental study, CAP and VOR were received from Arasto Pharmaceutical Chemicals Inc. (Iran). Dimethyl sulfoxide (DMSO), Tween 80, chloroform, PEG 600 and ethanol absolute were purchased from Scharlau (Spain) or Merck (Germany). Castor oil, trypan blue and 3-(4,5-dimethylthiazol-2-yl)-2,5-diphenyltetrazolium bromide (MTT) were bought from Sigma (USA). PANC1 (NCBI C556), MCF7 (NCBI C135), and HeLa (NCBI C115) cell lines were prepared from Pasteur Institute Cell Bank of Iran. For cell culture, Roswell Park Memorial Institute-1640 (RPMI 1640) was obtained from Shell max (Iran). Fetal bovine serum (FBS) was prepared

from Gibco (USA). Penicillin-streptomycin mixture was prepared from Danesh Azma Cell (Iran), and trypsin-EDTA were purchased from MedChem Express (China).

Construction of a ternary phase diagram

A ternary phase diagram was constructed by a titration method, while PEG 600, castor oil and Tween 80 were employed as cosurfactant, oil and surfactant. In brief, desired weights of the cosurfactant and surfactant were mixed in test tubes and mixed by a vortex to attain homogenized and clear solutions. Under magnetic stirring, oil was added dropwise until the mixture became turbid. The component amounts were converted to weight (%). Using the data, a ternary phase diagram was plotted where the top apex of the diagram was for the oil and the other sides were for cosurfactant and surfactant. The shadow area in the diagram shows the biphasic regains.

Formulations preparation

Two SNEDDSs with different ratios of the components were prepared inside the single-phase region of the phase diagram and symbolized as S1 and S2 (Figure 1 and Table 1). These formulations were selected to contain minimum amount of surfactant to attain a minimum cytotoxicity (vide infra). Blank SNEDDSs (S1-SNEDDS and S2-SNEDDS, vide infra) were prepared by mixing PEG 600, castor oil and Tween 80 by mixing for 1 min, dilution with distilled water (1:10), and mixing. The drug loaded SNEDDSs (S1-SNEDDS-CAP and S2-SNEDDS-VOR, vide infra) were similarly prepared in which the drugs were firstly mixed with the oil. The required weights of surfactant and cosurfactant were then added and shaken.

Formulations characterization

The SNEDDSs droplet size was determined by a particle size analyzer of Qudix, Scatterscope I (South Korea) in which the mean size

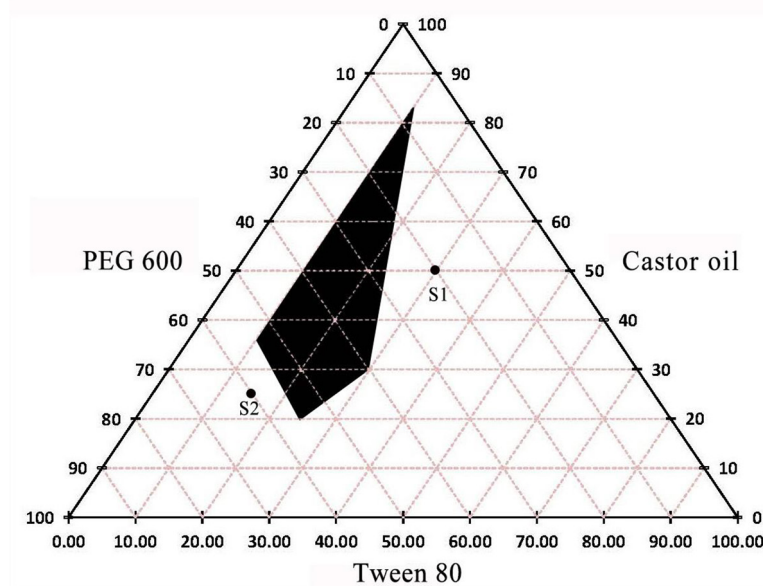


Figure 1: A ternary phase diagram for castor oil, tween 80 and polyethylene glycol (PEG) 600.

Table 1: Composition of formulations selected from ternary phase diagram.

Composition (W/W %)	S1	S2
Castor oil	50	25
Tween 80	30	15
Polyethylene Glycol (PEG) 600	20	60

was determined as $(D_{90}+D_{10})/2$, and its standard deviation was calculated as $(D_{90}-D_{10})/4$, that D_i denotes the droplet percentage with a size smaller than i . As indicator of polydispersity, span values were also obtained for the formulations as $(D_{90}-D_{10})/D_{50}$.

For FESEM sample preparation, one drop of a SNEDDS was dropped on a glass slide and then stained with OsO_4 . FESEM micrographs were captured by a TESCAN Mira 3-XMU (Czech Republic).

Stability of the formulations

S1-SNEDDS and S2-SNEDDS as well as S1-SNEDDS-CAP and S2-SNEDDS-VOR were stored in vials in dark at room

temperature for 30 days, and macroscopic features of these formulations were investigated.

Drug quantitation by high-performance liquid chromatography (HPLC)

Samples of CAP and VOR were analyzed by HPLC on a Waters instrument (USA) equipped with a UV/Vis detector using a C18 column from Eurospher (Germany, 5 μ m, 4.6 mm \times 250 mm). The mobile phase for CAP analysis contained a methanol/acetonitrile/water mixture of 80:18:2 ratios (V/V), and for VOR was a methanol/acetonitrile/water mixture of 70:28:2 ratios (V/V), pumped isocratically at 1.0 mL min⁻¹. The mobile phase was filtered via a 0.22 μ m Millipore membrane filter and degassed with a sonicator of Wise Clean (Germany) for 5 min before use. The injection volume was 60 μ L, the retention time was 3.2 \pm 0.08 and 3.03 \pm 0.01 min for CAP and VOR, respectively. CAP and VOR were detected at 272 and 260 nm, respectively, at 25 $^{\circ}$ C. Standard curves were firstly constructed for the drugs to quantify their contents in the corresponding samples. All values were reported as mean \pm standard deviation.

Entrapment efficiency and loading capacity

Entrapment efficiency (EE) and loading capacity (LC) were calculated using the equations:

$$EE = \text{Weight of drug loaded} / \text{Weight of drug added} \quad (1)$$

$$LC = \text{Weight of drug loaded} / \text{Weight of SNEDDS} \quad (2)$$

20 mg CAP and VOR, separately, were dissolved into 2.5 mL of SNEDDS. Then the drugs were separated from the formulations by liquid-liquid extraction by adding 1.0 mL chloroform and shaking for 5 min. The organic liquid was then separated and its CAP or VOR concentration was determined by HPLC in triplicate determinations.

Determination of drug release from the formulations

The release profiles of the drugs from SNEDDS were determined using dialysis bags. First, 2.5 mL of S1-SNEDDS-CAP or S2-SNEDDS-VOR containing 15 mg drug was placed in a dialysis tube (12000 MWCO). Next, the dialysis tube was suspended in 25 mL of a release medium containing an ethanol/water mixture of 70:30 ratio (V/V) in a beaker to obey the sink conditions. The beaker was maintained at room temperature under stirring at 100 rpm. Aliquots of 0.5 mL were separated at desired times, and the same amounts of medium were replaced to keep the total volume constant. Drug concentrations were determined using HPLC and pre-plotted calibration curves with triplicate measurements.

Cell culture and cytotoxicity assay

Cytotoxicity of the formulations was evaluated in vitro by the MTT assay on HeLa, PANC1 and MCF7 cells. In brief, the cells were cultured in cell culture flasks in RPMI-1640 medium with 1% penicillin/streptomycin and 10% fetal bovine serum. The cells were incubated at 37 °C and an air atmosphere containing 5% CO₂. Confluent cultures were trypsinized and employed for cytotoxicity

assessment. The cells were seeded in 96-well plates at 2×10^4 cells well⁻¹. 10 µL of different concentrations of CAP-SNEDDS or VOR-SNEDDS was then added independently to provide final concentrations of 0.024 to 25 µg mL⁻¹. Parallel sets were prepared without drug under the same conditions and served as controls. The plates were then incubated for 24 h followed by addition of 10 µL of a MTT solution of 5 mg mL⁻¹ in phosphate buffer saline (PBS, 100 mmol L⁻¹, pH 7.4) into each well. The plates were located for 4 h in dark. The generated formazan product was quantified at 570 nm using a microplate reader of BioTek (USA). For the non-treated control cells the viability was considered as 100%. Each measurement was replicated five times.

Analysis of apoptosis by terminal deoxynucleotidyl transferase-mediated terminal deoxynucleotidyl transferase (dUTP) nick end labeling (TUNEL) assay

DNA fragmentation due to apoptosis was evaluated by a kit of apoptosis detection of Takara (Japan) based on the TUNEL assay. In this assay, fragmentation of DNA was discerned by terminal labeling of the 3'-hydroxyl termini of the break sites of DNA resulting from activation of apoptotic of intracellular endonucleases. Fluorescein-dUTP combines into the ends of broken DNA segments, and then is detected with fluorescence microscopy. TUNEL analysis was done to evaluate apoptosis in the PANC1, HeLa and MCF7 cells in the presence of S1-SNEDDS-CAP or S2-SNEDDS-VOR, according to the manufacturer's instruction. TUNEL apoptotic cells of tumors in different groups were appeared green. While the blue color of 4',6-diamidino-2-phenylindole (DAPI) indicated all the cells, the green color showed apoptotic cells.

The cells were seeded in the plates and treated with S1-SNEDDS-CAP or S2-SNEDDS-VOR for 24 h. The medium was then removed, and the cells were washed with PBS followed

by fixing with a paraformaldehyde solution 4% for 0.5 h. After rinsing with PBS, the cells were processed with the permeation solution for about 5 min at 4 °C. The cells were washed again with PBS and incubate with 50 μ L of the labeling mixture for 90 min in a humidified atmosphere. Lastly, the cells were stained with DAPI and observed by a fluorescence microscope of Olympus (Japan).

Statistical analysis

The quantities are reported as means \pm standard deviation. For multiple comparisons, significant differences were tested by Student's t-test. *P*-value of <0.05 was considered for significant differences.

Results

A constructed ternary phase diagram for PEG 600, castor oil and Tween 80 is depicted in Figure 1. The shaded regions in the diagram indicate biphasic areas, and the other parts represent monophasic ones. Upon dilution of the components with ratios chosen from the monophasic regions, isotropic, clear and transparent nanoemulsions are formed. In the present study, two formulations were chosen from this region with lower amounts of the surfactant and higher concentrations of the cosurfactant and oil. These formulations were symbolized as S1 and S2 and the component ratios are depicted in Table 1. Because CAP is relatively more hydrophobic and VOR is relatively more hydrophilic (based on their solubility values in water), we choose S1-SNEDDS for loading CAP, and S2-SNEDDS for loading VOR. This is due to higher/lower oil content of S1/S2 formulation.

The mean the droplet size of the S1 and S2 formulations following dilution with 10 volume times of water and formation of the corresponding SNEDDS (denoted by S1-SNEDDS and S2-SNEDDS), and the mean droplet sizes of the S1-SNEDDS and S2-SNEDDS formulations upon CAP and VOR loading, respectively (denoted as S1-SNEDDS-CAP and

S2-SNEDDS-VOR), were determined by dynamic light scattering (Figure 2) and demonstrated in Table 2.

FESEM micrographs captured from S1-SNEDDS and S2-SNEDDS (Figure 3) showed different morphologies. In the former, particles are seemed with a smooth surface, a near spherical shape and a mean particle size of 138 ± 20 nm. In the latter, however, particles with a rough surface are observed with a mean size of 75 ± 21 nm (the particle sizes are also reported in Table 2).

Regarding storage times (stability) of SNEDDSs, it should be mentioned that no

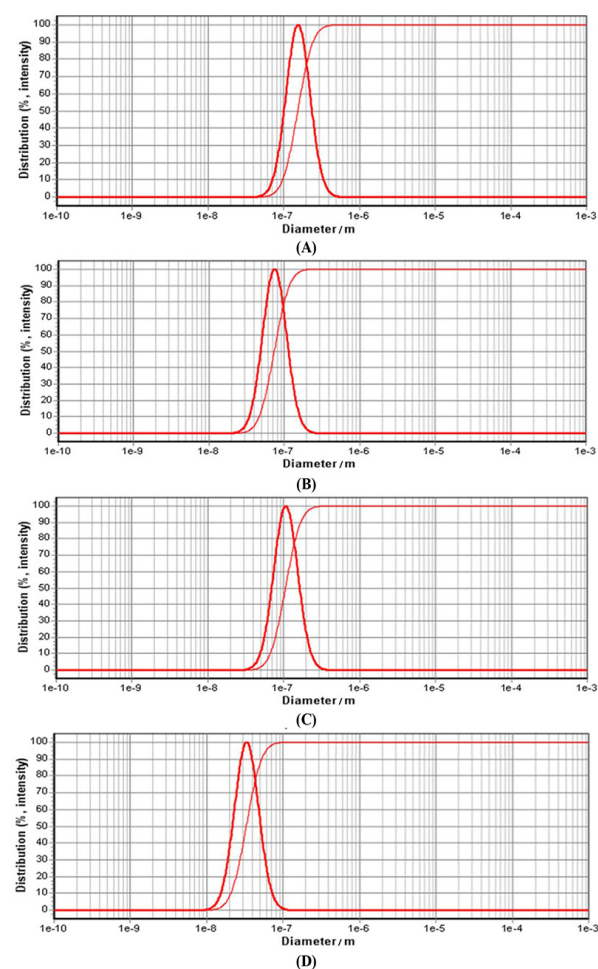


Figure 2: Size distribution diagrams for Self-nanoemulsifying drug delivery systems (SNEDDS) S1-SNEDDS (A), S2-SNEDDS (B), S1-SNEDDS-CAP (capecitabine) (C) and S2-SNEDDS-VOR (vorinostat) (D).

Table 2: Droplet sizes and span values for SNEDDSs containing ratios (in weight) of castor oil:Tween 80:PEG 600 of 50:30:20 (S1-SNEDDS) and 25:15:60 (S2-SNEDDS), and self-nanoemulsifying drug delivery system loaded with capecitabine (S1-SNEDDS-CAP) and self-nanoemulsifying drug delivery system loaded with vorinostat (S2-SNEDDS-VOR) obtained by particle size analysis (PSA) and field emission scanning electron microscopy (FESEM).

Formulation	Droplet size / nm (PSA)	Span value (PSA)	Droplet size / nm (FESEM)
S1-SNEDDS	171±37	0.96	138±20
S2-SNEDDS	82±18	0.95	75±21
S1-SNEDDS-CAP	117±26	0.97	-
S2-SNEDDS-VOR	37±8	0.96	-

PSA: Particle Size Analysis, FESEM: Field Emission Scanning Electron Microscopy

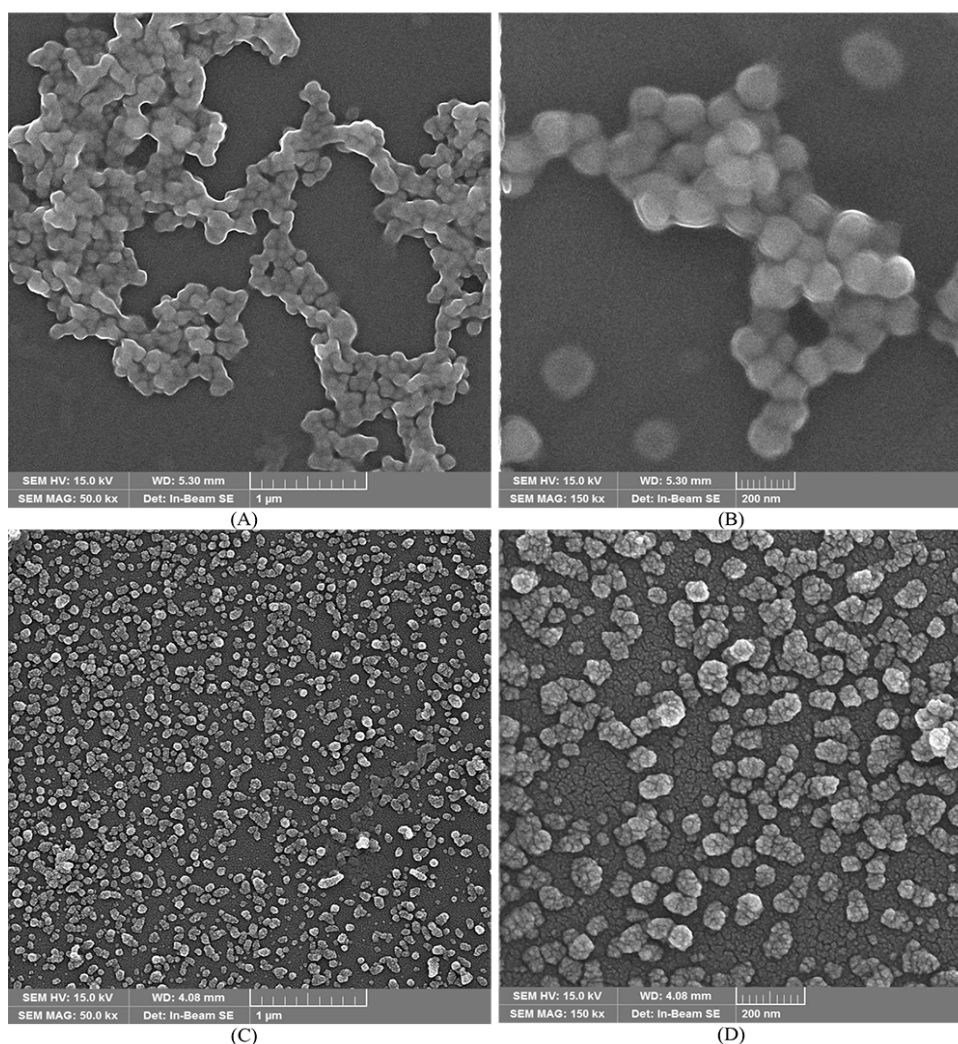


Figure 3: Field emission scanning electron microscopy (FESEM) images of SNEDDSs containing ratios (in weight) of castor oil:Tween 80:polyethylene glycol (PEG) 600 of 50:30:20 (S1-SNEDDS, **A, B**) and 25:15:60 (S2-SNEDDS, **C, D**) at different magnifications.

phase separation was occurred in all of the formulations at least for 30 days, inferring stability of the nanoformulations.

To measure EE and LC of CAP and VOR in S1-SNEDDS and S2-SNEDDS, and their release from the S1-SNEDDS-CAP and S2-SNEDDS-VOR, calibration curves for quantitation of the drugs were firstly plotted (Figure 4). Based on the data and calibration curves, CAP and VOR were determined by the figure of merits presented in Table 3. Using the results, EE of S1-SNEDDS-CAP and S2-SNEDDS-VOR are 19.4 ± 3.3 and $16.7\pm 3.9\%$, respectively. In addition, LC of S1-SNEDDS-CAP and S2-SNEDDS-VOR were obtained as 15.5 ± 2.6 and $13.4\pm 3.1\%$ respectively. Release patterns of CAP and VOR from S1-SNEDDS-CAP and S2-SNEDDS-VOR are shown in Figure 5. For both formulations, initial burst releases were observed for about 1 h, the release rates were then decreased and a steady state was attained after <6 h. In comparison, CAP was released from S1-SNEDDS-CAP with a higher rate. This higher release rate is related to higher solubility of CAP in the release medium due to more hydrophobicity (*vide supra*).

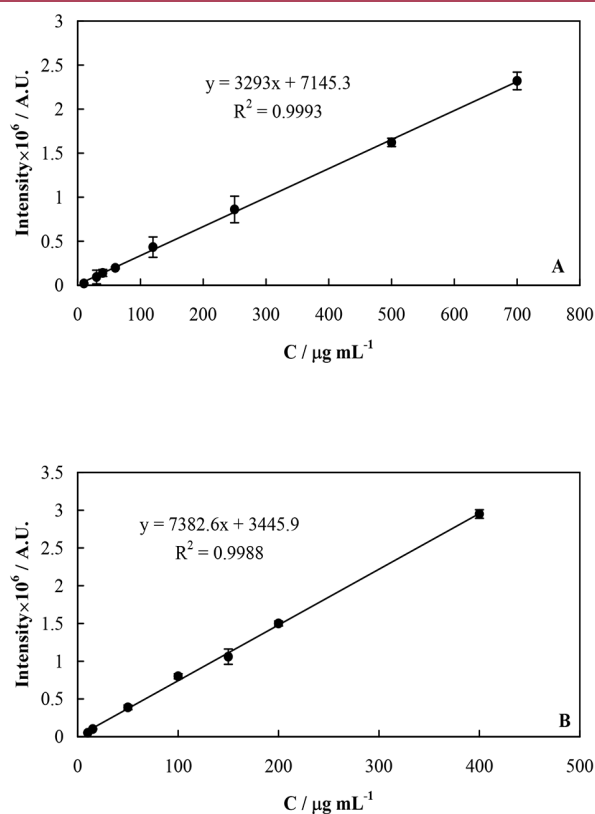


Figure 4: Calibration curves for quantitation of capecitabine (CAP, **A**) and vorinostat (VOR, **B**) obtained by high-performance liquid chromatography (HPLC).

Table 3: Determined parameters of capecitabine (CAP) and vorinostat (VOR) by high-performance liquid chromatography (HPLC).

	CAP	VOR
Regression equation	$y=(3293\pm 35.8)x + (7145.3\pm 11488.4)$	$y=(7382.6\pm 115.0)x + (3445.9\pm 21093.9)$
R ²	0.9993	0.9988
Linear concentration range / $\mu\text{g mL}^{-1}$	10-700	10-400
Relative standard deviation (RSD)%	^a 3.9	^b 4.7
^c Limit of detection (LOD) / $\mu\text{g mL}^{-1}$	2.5	2.0
^d Limit of detection (LOQ) / $\mu\text{g mL}^{-1}$	8.3	6.6

VOR: Vorinostat, CAP: Capecitabine

^aRelative standard deviation for a concentration of $50 \mu\text{g mL}^{-1}$

^bRelative standard deviation for a concentration of $40 \mu\text{g mL}^{-1}$

^cLimit of detection equal to $3\times\text{SD}/B$, where SD is the standard deviation of the blank signal, and B is the slope of the calibration curve

^dLimit of quantitation equal to $10\times\text{SD}/B$, where SD is the standard deviation of the blank signal, and B is the slope of the calibration curve

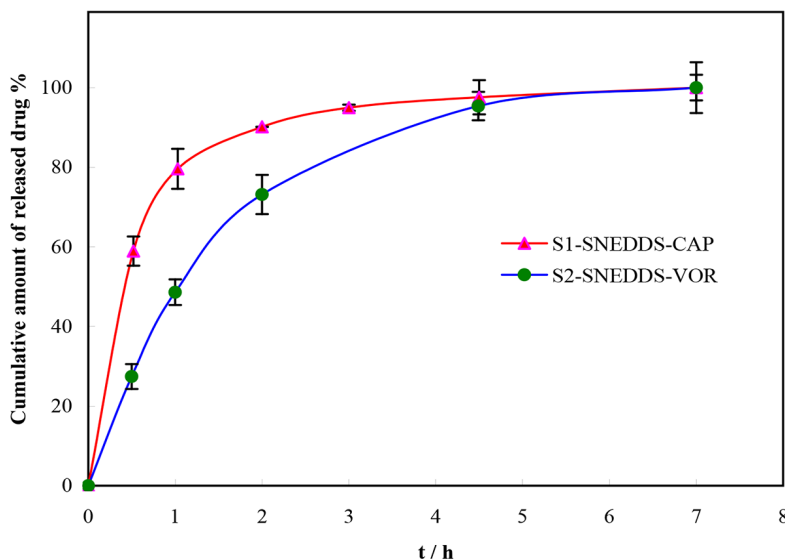


Figure 5: Release patterns of capecitabine (CAP) and vorinostat (VOR) from self-nanoemulsifying drug delivery system loaded with capecitabine (S1-SNEDDS-CAP) and self-nanoemulsifying drug delivery system loaded with vorinostat (S2-SNEDDS-VOR).

The cell viability of S1-SNEDDS-CAP against MCF7 and PANC1 cell lines and S2-SNEDDS-VOR against MCF7 and HeLa cell lines both in a concentration range of 0.024-25 μM were evaluated as shown in Figure 6. Figures 6A and B represent the viability of the MCF7 and PANC1 cells reduced to about 72% in the presence of S1-SNEDDS alone without any drug, which demonstrates a significant difference with the control cells. Also, Figures 6C and D show the viability of MCF7 and HeLa cells upon treatment with S2-SNEDDS formulation without any drug was about 86% with no significant difference with the viability of control cells. Therefore, S2-SNEDDS formulation induced much less toxicity and higher biocompatibility compared to S1-SNEDDS formulation in these cells.

Comparison of the viabilities of PANC1 and MCF7 cell lines in the presence of different concentration of CAP in the suspension form and in the S1-SNEDDS formulation (0.024-25 $\mu\text{g mL}^{-1}$) are presented in Figures 6A and B. As shown in the Figures 6A and B, CAP in the S1-SNEDDS formulation is much more effective with very significant difference in

killing the cells compared to suspension form. Even 0.024 $\mu\text{g mL}^{-1}$ CAP in S1-SNEDDS reduced MCF7 and PANC1 cell viability to about 11.9% and 38.4%, whereas equal amount of CAP in suspension, with 100% viability do not effect on the cells. Increasing concentrations of CAP in S1-SNEDDS from 0.024 to 25 $\mu\text{g mL}^{-1}$ did not decrease the viability of MCF7 and PANC1 cells. From these results, half-maximal inhibitory concentration (IC_{50}) values for CAP suspension and S1-SNEDDS-CAP toward MCF7 cells were estimated as 16 and $<0.024 \mu\text{g mL}^{-1}$, respectively. Also, IC_{50} values for CAP suspension and S1-SNEDDS-CAP toward PANC1 cells were estimated as 167 and $<0.024 \mu\text{g mL}^{-1}$, respectively.

These more confirmed the effectiveness of the SNEDDS formulation. The cell viabilities of MCF7 and HeLa upon treatment with different VOR concentrations in the suspension form and S2-SNEDDS-VOR (0.024-25 $\mu\text{g mL}^{-1}$) were evaluated and are shown in Figures 6C and D, respectively. The viability of cells in the presence of VOR in these concentrations did not show any significant difference with untreated control cells. Also,

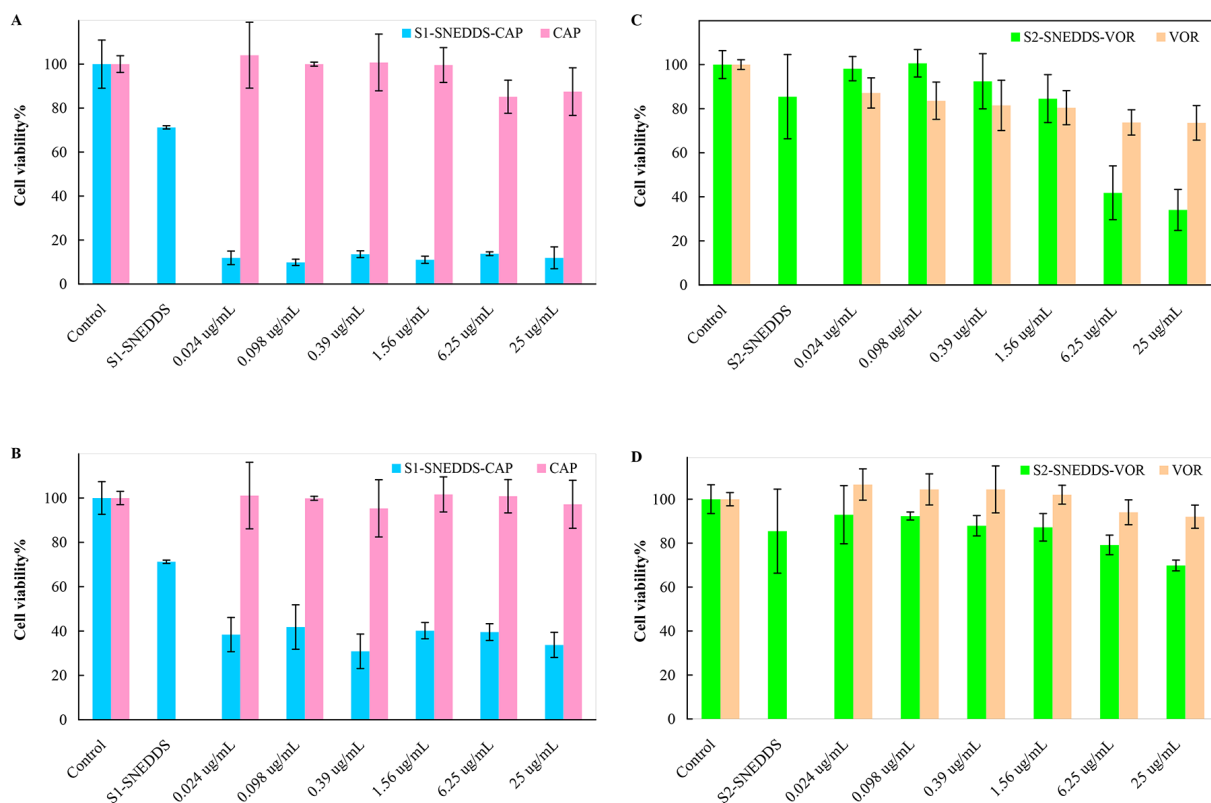


Figure 6: The cell viability of self-nanoemulsifying drug delivery system loaded with capecitabine (S1-SNEDDS-CAP) against MCF7 (A) and PANC1 (B) cell lines, and self-nanoemulsifying drug delivery system loaded with vorinostat (S2-SNEDDS-VOR) against MCF7 (C) and HeLa (D) cell lines in a concentration range of 0.024–25 μM .

S2-SNEDDS-VOR until 1.56 $\mu\text{g mL}^{-1}$ did not have significant effect on decreasing cell viability. However, S2-SNEDDS-VOR at 6.25 and 25 $\mu\text{g mL}^{-1}$ reduced MCF7 cell viability to less than 40%. On the other hand, only 25 $\mu\text{g mL}^{-1}$ of S2-SNEDDS-VOR showed significant effect in killing HeLa cells. From these results, IC_{50} values for VOR suspension and S2-SNEDDS-VOR toward MCF7 cells were obtained as 14 and 5.3 $\mu\text{g mL}^{-1}$, respectively. Also, IC_{50} values for VOR suspension and S2-SNEDDS-VOR toward HeLa cells were obtained as 20 and 11.3 $\mu\text{g mL}^{-1}$, respectively. Therefore, formulation of nanoemulsion and the type of cancer cell are significant in the outcome of the viability results. Nonetheless, these results demonstrate considerable improvements in the effectiveness of

CAP and VOR as anticancer drugs on tumor cells upon incorporation into SNEDDSs. In Table 4, information regarding the CAP- and VOR-affecting cell lines (with or without a carrier) has been summarized that indicated the efficacy of CAP and VOR on different cancer cell lines.

Cell apoptosis induction by chemotherapeutic drugs is one of the best routes for cancer treatment. Cell apoptosis is a programmed cell death mechanism that takes place via intrinsic or extrinsic pathways [45]. While in extrinsic pathway, various ligands bind with tumor necrosis factors, and lead to this factor to death and cell apoptosis, cellular processes such as DNA damage, oxidative stress and acting of cytotoxic agents lead to apoptosis via the intrinsic pathway [45].

Table 4: Cytotoxicity of capecitabine (CAP) and vorinostat (VOR) toward cancer cell lines.

Drug	Carrier	Cell lines	Half-maximal inhibitory concentration (IC50)	Ref.
VOR	Polymeric nanoparticles	Pleural mesothelial cell line	100 $\mu\text{mol L}^{-1}$	[14]
VOR	-	Cutaneous T-cell lymphoma	2.062 $\mu\text{mol L}^{-1}$	[29]
VOR	-	Human gastric cancer cell line	5.76 $\mu\text{mol L}^{-1}$	[30]
VOR	-	Hep-2 cell line	3 $\mu\text{mol L}^{-1}$	[31]
VOR	-	Breast cancer cell line	2.5 nmol L^{-1}	[32]
VOR	Drug-incorporated nanoparticles	HuCC-T1 human cholangiocarcinoma cells	-	[33]
VOR	Nanoparticles	HepG2 cell line	6.30 \pm 0.59 $\mu\text{mol L}^{-1}$	[34]
VOR	Solid lipid nanoparticles	(MCF-7, A549, and MDA-MB-231)	-	[35]
CAP	-	Colon cancer cell line	6.5 mg mL^{-1}	[36]
CAP	-	Gastric cancer cell lines	16.45 \pm 1.22 $\mu\text{g L}^{-1}$	[37]
CAP	-	Colon cancer cell line	3.27 \pm 0.42 $\mu\text{mol L}^{-1}$	[38]
CAP	-	Colon cancer cell line	1.63 \pm 0.33 $\mu\text{mol L}^{-1}$	[38]
CAP	Polymeric nanoparticles	HepG2 cell line	101 \pm 20.21 $\mu\text{g mL}^{-1}$	[7]
CAP	Nano erythroosome	-	-	[39]
CAP	Nanomicelle	-	-	[40]
CAP	Polymeric nanoparticles	-	-	[41]

VOR: Vorinostat, CAP: Capecitabine

Figure 7 shows the obtained results of TUNEL assay in the presence of S1-SNEDDS-CAP or S2-SNEDDS-VOR in the cells. It was observed that after treatment the cells with the formulations, number of cells of TUNEL positive was significantly raised indicating a significant apoptosis in all the cells. These results approved the efficacy of S1-SNEDDS-CAP and S2-SNEDDS-VOR.

Discussion

To choose the SNEDDS components, the following situations were considered: a) Safety is a key factor to select the components. Because toxicity of nonionic surfactants is lower (than the ionic surfactants), Tween 80 was selected. On the other hand, surfactants represent the major cytotoxicity of the drug formulations [46], and therefore, the surfactant ratio in the SNEDDS formations was selected

to be as low as possible as 30% (W/W). b) The value of hydrophilic-lipophilic balance (HLB) for a surfactant for formation of nanoemulsion of oil-in-water should be >10 [47]. HLB value for Tween 80 is 15, and therefore, this surfactant is a good choice. c) A cosurfactant that is usually employed acts as an adjuvant of the main surfactant to further reduction of the interfacial tension and must be miscible with the oil and surfactant. d) Mixing of the SNEDDS components must lead to formation of a single phase, and after addition in water, a stable nanoemulsion must be prepared. One of the appropriate routes for selection of suitable amounts of components to create nanoemulsions is the construction of ternary phase diagrams. Within the single-phase region of such the diagram, self-nanoemulsifying process is performed with minimum free energy. Therefore, emulsifying process will be

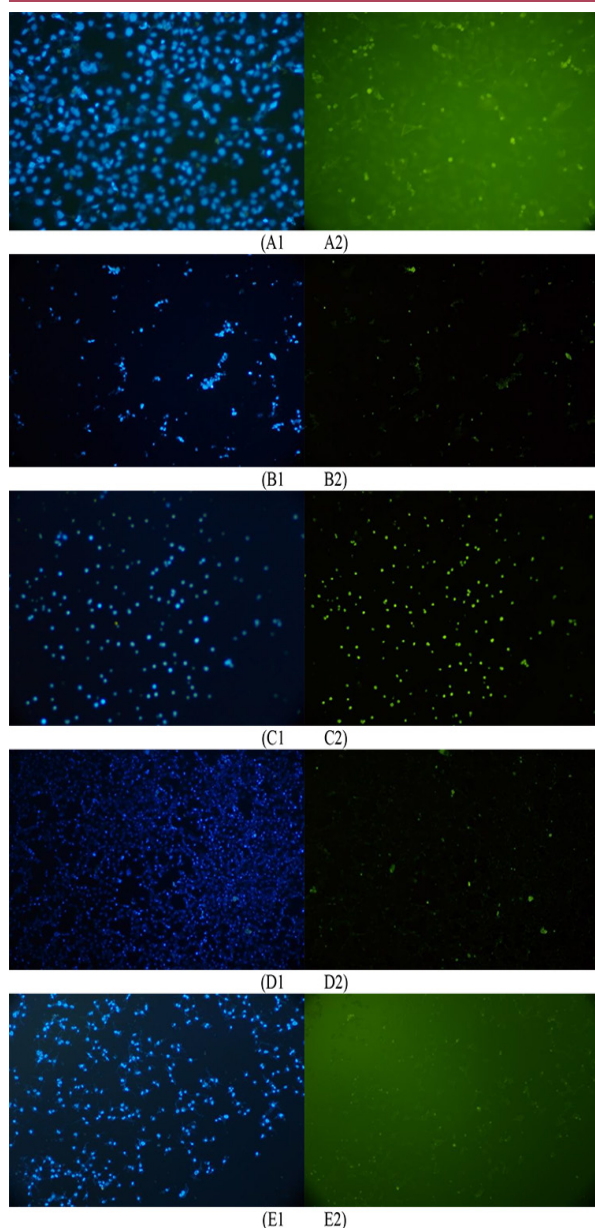


Figure 7: The terminal deoxynucleotidyl transferase-mediated terminal deoxynucleotidyl transferase (dUTP) nick end labeling (TUNEL) assay results obtained for the effect of control (**A1** and **A2**), self-nanoemulsifying drug delivery system loaded with capecitabine (S1-SNEDDS-CAP) on MCF7 (**B1** and **B2**), S1-SNEDDS-CAP on PANC1 (**C1** and **C2**), self-nanoemulsifying drug delivery system loaded with vorinostat (S2-SNEDDS-VOR) on MCF7 (**D1**, **D2**) and S2-SNEDDS-VOR on HeLa (**E1**, **E2**) cell lines.

thermodynamically spontaneous. According to the results, the formulation with higher oil ratio (S1, two times higher weight of oil) contained larger droplets of oil (about two times bigger oil droplets) with lower ratios of surfactant and cosurfactant surrounding the surface of droplets of oil. On the other hand, the mean droplet sizes of the formulations S1-SNEDDS-CAP and S2-SNEDDS-VOR indicated domination of strong attraction forces between CAP/VOR and the oil droplet components. These forces lead to considerable decrease in the droplet size after drug loading. The differences between the hydrodynamic sizes obtained by dynamic light scattering and droplet sizes obtained by FESEM can be related to sample preparation method in FESEM. It seems that S2-SNEDDS comprised finer droplets, compared to S1-SNEDDS, as it was evident from PSA, and each particle (droplet) contained adhered very smaller ones. The droplets were may be comprised dissolved surfactant and/or cosurfactant into the droplets and are observed as adhered nanoparticles. SNEDDSs improve drug efficacy by increment in the solubility, facilitation of drug lymphatic transport, protection from degradation, inhibition the P-glycoprotein mediated multidrug efflux [48, 49], and controlling and sustaining delivery [50]. The growth inhibition effect of the formulations was due to the apoptosis induction. CAP and VOR induce cell cycle arrest and activation of caspases [51], and TUNEL positive cells resulted from DNA fragmentation induced DNA damage associated with caspase-dependent activation of apoptosis.

Conclusion

SNEDDSs have been widely examined to improve oral bioavailability of different drugs. In the present study, two optimized SNEDDSs were prepared using a natural lipid and suitable excipients. Cater oil employed in our formulation is an ideal component of SNEDDSs because of its availability, low cost and safety. The solubilizing ability of the cosurfactant

and surfactant is also a key parameter for successful loading into SNEDDSs and in vivo efficacy of the drugs. The optimized SNEDDSs comprised stable homogenous and spherical nanodroplets with good EEs and LCs. The drug-loaded SNEDDSs showed improved anticancer activity, compared to the drug themselves. SNEDDS with promising in vitro characters can apply as a new delivery system for the oral delivery of drugs such as CAP and VOR. The results presented above thoroughly presented higher effectiveness of the SNEDDS formulations as compared to the drugs alone.

Acknowledgment

We would like to thank the Research Council of Shiraz University of Medical Science for supporting this research (14723).

Authors' Contribution

R. Nazari-Vanani performed all the experiments and wrote the original draft of the paper. N. Sattarahmady participated in the idea development, prepared some figures and provided some parts of the discussions. K. Karimian provided some supports and analyzed the results. H. Heli participated in the idea development and supervised the study. All the authors read, modified, and approved the final version of the manuscript.

Ethical Approval

The national ethics committee confirmed the study with the ethical code 1396-01-57-14723. We did not perform any intervention in therapeutic procedures. Therefore, gathering the consent forms was waived due to the nature of this study.

Funding

This work was supported by Shiraz University of Medical Sciences (Shiraz, Iran) with the grant number "1396-01-57-14723 (11648)".

Conflict of Interest

None

References

1. Ali I, Rahis-Uddin, Salim K, Rather MA, Wani WA, Haque A. Advances in nano drugs for cancer chemotherapy. *Curr Cancer Drug Targets*. 2011;**11**(2):135-46. doi: 10.2174/156800911794328493. PubMed PMID: 21158724.
2. Allen TM, Cheng WW, Hare JI, Laginha KM. Pharmacokinetics and pharmacodynamics of lipidic nano-particles in cancer. *Anticancer Agents Med Chem*. 2006;**6**(6):513-23. doi: 10.2174/187152006778699121. PubMed PMID: 17100556.
3. De La Cruz L, Blankenship SA, Chatterjee A, Geha R, Nocera N, Czerniecki BJ, et al. Outcomes After Oncoplastic Breast-Conserving Surgery in Breast Cancer Patients: A Systematic Literature Review. *Ann Surg Oncol*. 2016;**23**(10):3247-58. doi: 10.1245/s10434-016-5313-1. PubMed PMID: 27357177.
4. Van Cutsem E, Findlay M, Osterwalder B, Kocha W, Dalley D, Pazdur R, et al. Capecitabine, an oral fluoropyrimidine carbamate with substantial activity in advanced colorectal cancer: results of a randomized phase II study. *J Clin Oncol*. 2000;**18**(6):1337-45. doi: 10.1200/JCO.2000.18.6.1337. PubMed PMID: 10715306.
5. Vainchtein LD, Rosing H, Schellens JH, Beijnen JH. A new, validated HPLC-MS/MS method for the simultaneous determination of the anti-cancer agent capecitabine and its metabolites: 5'-deoxy-5-fluorocytidine, 5'-deoxy-5-fluorouridine, 5-fluorouracil and 5-fluorodihydrouracil, in human plasma. *Biomed Chromatogr*. 2010;**24**(4):374-86. doi: 10.1002/bmc.1302. PubMed PMID: 19650151.
6. Devanaboyina N, Kishore YS, Pushpalatha P, Mammatha N, Venkatesh P. Development and validation of new RP HPLC method for analysis of capecitabine in pharmaceutical dosage form. *Int J Sci Invent Today*. 2013;**2**(1):21-30.
7. Sun SB, Liu P, Shao FM, Miao QL. Formulation and evaluation of PLGA nanoparticles loaded capecitabine for prostate cancer. *Int J Clin Exp Med*. 2015;**8**(10):19670-81. PubMed PMID: 26770631. PubMed PMCID: PMC4694531.
8. Woods DM, Woan K, Cheng F, Wang H, Perez-Villarroel P, Lee C, et al. The antimelanoma activity of the histone deacetylase inhibitor panobinostat (LBH589) is mediated by direct tumor cytotoxicity and increased tumor immunogenicity. *Melanoma Res*. 2013;**23**(5):341-8. doi: 10.1097/CMR.0b013e328364c0ed. PubMed PMID: 23963286. PubMed PMCID: PMC4012016.
9. Carew JS, Giles FJ, Nawrocki ST. Histone deacety-

- lase inhibitors: mechanisms of cell death and promise in combination cancer therapy. *Cancer Lett.* 2008;**269**(1):7-17. doi: 10.1016/j.canlet.2008.03.037. PubMed PMID: 18462867.
10. Khan O, La Thangue NB. HDAC inhibitors in cancer biology: emerging mechanisms and clinical applications. *Immunol Cell Biol.* 2012;**90**(1):85-94. doi: 10.1038/icb.2011.100. PubMed PMID: 22124371.
 11. Chidambaram M, Manavalan R, Kathiresan K. Nanotherapeutics to overcome conventional cancer chemotherapy limitations. *J Pharm Pharm Sci.* 2011;**14**(1):67-77. doi: 10.18433/j30c7d. PubMed PMID: 21501554.
 12. Ajdari M, Ranjbar A, Karimian K, Karimi M, Heli H, Sattarahmady N. Characterization and Evaluation of Nano-niosomes Encapsulating Docetaxel against Human Breast, Pancreatic, and Pulmonary Adenocarcinoma Cancer Cell Lines. *J Biomed Phys Eng.* 2024;**14**(2):159-68. doi: 10.31661/jbpe.v0i0.2401-1708. PubMed PMID: 38628892. PubMed PMCID: PMC11016824.
 13. Nazari-Vanani R, Sattarahmady N, Heli H. Nanotechnological approaches for enhancing the oral bioavailability of curcumin. *J Biol Today's World.* 2017;**6**(7):129-32. doi: 10.15412/J.JBTW.01060702.
 14. Denis I, El Bahhaj F, Collette F, Delatouche R, Gueugnon F, Pouliquen D, et al. Vorinostat-polymer conjugate nanoparticles for Acid-responsive delivery and passive tumor targeting. *Biomacromolecules.* 2014;**15**(12):4534-43. doi: 10.1021/bm501338r. PubMed PMID: 25333409.
 15. Negahdary M, Behjati-Ardakani M, Sattarahmady N, Yadegari H, Heli H. Electrochemical aptasensing of human cardiac troponin I based on an array of gold nanodumbbells-Applied to early detection of myocardial infarction. *Sens Actuators B Chem.* 2017;**252**:62-71. doi: 10.1016/j.snb.2017.05.149.
 16. Ajdari MR, Tondro GH, Sattarahmady N, Parsa A, Heli H. Phytosynthesis of silver nanoparticles using *Myrtus communis* L. leaf extract and investigation of bactericidal activity. *J Electron Mat.* 2017;**46**:6930-5. doi: 10.1007/s11664-017-5784-2.
 17. Dehdari Vais R, Yadegari H, Heli H, Sattarahmady N. A β -Amyloid(1-42) Biosensor Based on Molecularly Imprinted Poly-Pyrrole for Early Diagnosis of Alzheimer's Disease. *J Biomed Phys Eng.* 2021;**11**(2):215-28. doi: 10.31661/jbpe.v0i0.1070. PubMed PMID: 33937128. PubMed PMCID: PMC8064131.
 18. Dehdari Vais R, Yadegari H, Heli H. Synthesis of Flower-like Nickel Hydroxide Nanosheets and Application in Electrochemical Determination of Famotidine. *Iran J Pharm Res.* 2020;**19**(1):120-37. doi: 10.22037/ijpr.2019.14257.12245. PubMed PMID: 32922475. PubMed PMCID: PMC7462516.
 19. Negahdary M, Heli H. An electrochemical peptide-based biosensor for the Alzheimer biomarker amyloid- β (1-42) using a microporous gold nanostructure. *Mikrochim Acta.* 2019;**186**(12):766. doi: 10.1007/s00604-019-3903-x. PubMed PMID: 31713687.
 20. Negahdary M, Heli H. An electrochemical troponin I peptisensor using a triangular icicle-like gold nanostructure. *Biochem Eng J.* 2019;**151**:107326. doi: 10.1016/j.bej.2019.107326.
 21. Karimi M, Karimian K, Heli H. A nanoemulsion-based delivery system for imatinib and in vitro anti-cancer efficacy. *Braz J Pharm Sci.* 2021;**56**:e18973. doi: 10.1590/s2175-97902020000118973.
 22. Wang J, Li B, Qiu L, Qiao X, Yang H. Dendrimer-based drug delivery systems: history, challenges, and latest developments. *J Biol Eng.* 2022;**16**(1):18. doi: 10.1186/s13036-022-00298-5. PubMed PMID: 35879774. PubMed PMCID: PMC9317453.
 23. Papagiannaros A, Bories C, Demetzos C, Loiseau PM. Antileishmanial and trypanocidal activities of new miltefosine liposomal formulations. *Biomed Pharmacother.* 2005;**59**(10):545-50. doi: 10.1016/j.biopha.2005.06.011. PubMed PMID: 16325367.
 24. Nazari-Vanani R, Kayani Z, Karimian K, Ajdari MR, Heli H. Development of New Nanoniosome Carriers for Vorinostat: Evaluation of Anticancer Efficacy In Vitro. *J Pharm Sci.* 2024;**113**(8):2584-94. doi: 10.1016/j.xphs.2024.05.025. PubMed PMID: 38801974.
 25. Liu M, Du H, Zhai G. The Design of Amphiphilic Polymeric Micelles of Curcumin for Cancer Management. *Curr Med Chem.* 2015;**22**(38):4398-411. doi: 10.2174/092986732238151228191020. PubMed PMID: 26714503.
 26. Nasr A, Gardouh A, Ghorab M. Novel Solid Self-Nanoemulsifying Drug Delivery System (S-SNEDDS) for Oral Delivery of Olmesartan Medoxomil: Design, Formulation, Pharmacokinetic and Bioavailability Evaluation. *Pharmaceutics.* 2016;**8**(3):20. doi: 10.3390/pharmaceutics8030020. PubMed PMID: 27355963. PubMed PMCID: PMC5039439.
 27. Köllner S, Nardin I, Markt R, Griesser J, Prüfert F, Bernkop-Schnürch A. Self-emulsifying drug delivery systems: Design of a novel vaginal delivery system for curcumin. *Eur J Pharm Biopharm.* 2017;**115**:268-75. doi: 10.1016/j.ejpb.2017.03.012. PubMed PMID: 28323109.

28. Qian J, Meng H, Xin L, Xia M, Shen H, Li G, Xie Y. Self-nanoemulsifying drug delivery systems of myricetin: Formulation development, characterization, and in vitro and in vivo evaluation. *Colloids Surf B Biointerfaces*. 2017;**160**:101-9. doi: 10.1016/j.colsurfb.2017.09.020. PubMed PMID: 28917148.
29. Wozniak MB, Villuendas R, Bischoff JR, Aparicio CB, Martínez Leal JF, De La Cueva P, et al. Vorinostat interferes with the signaling transduction pathway of T-cell receptor and synergizes with phosphoinositide-3 kinase inhibitors in cutaneous T-cell lymphoma. *Haematologica*. 2010;**95**(4):613-21. doi: 10.3324/haematol.2009.013870. PubMed PMID: 20133897. PubMed PMCID: PMC2857191.
30. Huang C, Ida H, Ito K, Zhang H, Ito Y. Contribution of reactivated RUNX3 to inhibition of gastric cancer cell growth following suberoylanilide hydroxamic acid (vorinostat) treatment. *Biochem Pharmacol*. 2007;**73**(7):990-1000. doi: 10.1016/j.bcp.2006.12.013. PubMed PMID: 17276407.
31. Bruzzese F, Leone A, Rocco M, Carbone C, Piro G, Caraglia M, et al. HDAC inhibitor vorinostat enhances the antitumor effect of gefitinib in squamous cell carcinoma of head and neck by modulating ErbB receptor expression and reverting EMT. *J Cell Physiol*. 2011;**226**(9):2378-90. doi: 10.1002/jcp.22574. PubMed PMID: 21660961.
32. Wilson-Edell KA, Yevtushenko MA, Rothschild DE, Rogers AN, Benz CC. mTORC1/C2 and pan-HDAC inhibitors synergistically impair breast cancer growth by convergent AKT and polysome inhibiting mechanisms. *Breast Cancer Res Treat*. 2014;**144**(2):287-98. doi: 10.1007/s10549-014-2877-y. PubMed PMID: 24562770. PubMed PMCID: PMC4318538.
33. Kwak TW, Kim DH, Jeong YI, Kang DH. Antitumor activity of vorinostat-incorporated nanoparticles against human cholangiocarcinoma cells. *J Nanobiotechnology*. 2015;**13**:60. doi: 10.1186/s12951-015-0122-4. PubMed PMID: 26410576. PubMed PMCID: PMC4583727.
34. Han L, Wang T, Wu J, Yin X, Fang H, Zhang N. A facile route to form self-carried redox-responsive vorinostat nanodrug for effective solid tumor therapy. *Int J Nanomedicine*. 2016;**11**:6003-22. doi: 10.2147/IJN.S118727. PubMed PMID: 27956831. PubMed PMCID: PMC5113930.
35. Tran TH, Ramasamy T, Truong DH, Shin BS, Choi HG, Yong CS, Kim JO. Development of vorinostat-loaded solid lipid nanoparticles to enhance pharmacokinetics and efficacy against multidrug-resistant cancer cells. *Pharm Res*. 2014;**31**(8):1978-88. doi: 10.1007/s11095-014-1300-z. PubMed PMID: 24562809.
36. Kjellström J, Kjellén E, Johnsson A. In vitro radiosensitization by oxaliplatin and 5-fluorouracil in a human colon cancer cell line. *Acta Oncol*. 2005;**44**(7):687-93. doi: 10.1080/02841860500247552. PubMed PMID: 16227158.
37. Yuan F, Shi H, Ji J, Cai Q, Chen X, Yu Y, et al. Capecitabine metronomic chemotherapy inhibits the proliferation of gastric cancer cells through anti-angiogenesis. *Oncol Rep*. 2015;**33**(4):1753-62. doi: 10.3892/or.2015.3765. PubMed PMID: 25634241.
38. Mohammadian M, Zeynali S, Azarbaijani AF, Khadem Ansari MH, Kheradmand F. Cytotoxic effects of the newly-developed chemotherapeutic agents 17-AAG in combination with oxaliplatin and capecitabine in colorectal cancer cell lines. *Res Pharm Sci*. 2017;**12**(6):517-25. doi: 10.4103/1735-5362.217432. PubMed PMID: 29204180. PubMed PMCID: PMC5691578.
39. Payghan SA. Nanoengineered erythrovesicles: camouflaged capecitabine as a biomimetic delivery platform. *Asian J Pharm*. 2017;**11**(1):53-63. doi: 10.22377/ajp.v11i01.1044.
40. Zou F, Wei K, Peng X. Thermodynamics of micellization and sustained release of folate targeted capecitabine loaded nanomicelles. *J Nanosci Nanotechnol*. 2016;**16**(8):8519-27. doi: 10.1166/jnn.2016.12710.
41. Wei K, Peng X, Zou F. Folate-decorated PEG-PLGA nanoparticles with silica shells for capecitabine controlled and targeted delivery. *Int J Pharm*. 2014;**464**(1-2):225-33. doi: 10.1016/j.ijpharm.2013.12.047. PubMed PMID: 24463073.
42. Kwak TW, Lee HL, Song YH, Kim C, Kim J, Seo SJ, et al. Vorinostat-eluting poly(DL-lactide-co-glycolide) nanofiber-coated stent for inhibition of cholangiocarcinoma cells. *Int J Nanomedicine*. 2017;**12**:7669-80. doi: 10.2147/IJN.S141920. PubMed PMID: 29089762. PubMed PMCID: PMC5655133.
43. Akbari R, Javar HA. Efficacy of capecitabine and 5-fluorouracil (5-FU) on the human breast cancer cell line (MCF7)—effect of concentration. *Am J Res Commun*. 2013;**1**(16):75-91.
44. Tran TH, Choi JY, Ramasamy T, Truong DH, Nguyen CN, Choi HG, et al. Hyaluronic acid-coated solid lipid nanoparticles for targeted delivery of vorinostat to CD44 overexpressing cancer cells. *Carbohydr Polym*. 2014;**114**:407-15. doi: 10.1016/j.carbpol.2014.08.026. PubMed PMID: 25263908.
45. Ziegler DS, Kung AL. Therapeutic targeting of apoptosis pathways in cancer. *Curr*

- Opin Oncol.* 2008;**20**(1):97-103. doi: 10.1097/CCO.0b013e3282f310f6. PubMed PMID: 18043263.
46. Rebello S, Asok AK, Mundayoor S, Jisha MS. Surfactants: toxicity, remediation and green surfactants. *Environ Chem Lett.* 2014;**12**(2):275-87. doi: 10.1007/s10311-014-0466-2.
47. Shafiq S, Shakeel F, Talegaonkar S, Ahmad FJ, Khar RK, Ali M. Development and bioavailability assessment of ramipril nanoemulsion formulation. *Eur J Pharm Biopharm.* 2007;**66**(2):227-43. doi: 10.1016/j.ejpb.2006.10.014. PubMed PMID: 17127045.
48. Fracasso PM, Goldstein LJ, De Alwis DP, Rader JS, Arquette MA, Goodner SA, et al. Phase I study of docetaxel in combination with the P-glycoprotein inhibitor, zosuquidar, in resistant malignancies. *Clin Cancer Res.* 2004;**10**(21):7220-8. doi: 10.1158/1078-0432.CCR-04-0452. PubMed PMID: 15534095.
49. Sohail MF, Rehman M, Sarwar HS, Naveed S, Salman O, Bukhari NI, et al. Advancements in the oral delivery of Docetaxel: challenges, current state-of-the-art and future trends. *Int J Nanomedicine.* 2018;**13**:3145-61. doi: 10.2147/IJN.S164518. PubMed PMID: 29922053. PubMed PMID: PMC5997133.
50. Panyam J, Labhasetwar V. Biodegradable nanoparticles for drug and gene delivery to cells and tissue. *Adv Drug Deliv Rev.* 2003;**55**(3):329-47. doi: 10.1016/s0169-409x(02)00228-4. PubMed PMID: 12628320.
51. Li M, Zhang N, Li M. Capecitabine treatment of HCT-15 colon cancer cells induces apoptosis via mitochondrial pathway. *Trop J Pharm Res.* 2017;**16**(7):1529-36. doi: 10.4314/tjpr.v16i7.10.